Dynamic correlations in an electron gas. II. Kinetic-equation approach

P. K. Aravind, A. Holas,* and K. S. Singwi
Department of Physics and Astronomy, Northwestern University, Evanston, Illinois 60201
(Received 5 July 1979; revised manuscript received 16 July 1981)

Starting from the exact hierarchy of quantum kinetic equations for the Wigner distribution functions we develop a theory of dynamical correlations in an electron gas. By making a random-phase-approximation- (RPA) like truncation for the second equation in the hierarchy we obtain an expression for the proper polarizability of the form $Q=Q^0+Q^c$, where Q^0 is the Lindhard (RPA) function and Q^c is an additional term which has the following properties: (i) it includes all the three first-order Feynman diagrams for the proper polarizability, (ii) it incorporates in addition the coupled propagation of two particle-hole pairs, and (iii) it leads to an expression for the density-density response function which satisfies exactly the first- and third-frequency-moment sum rules. Detailed calculations of plasmon dispersion, damping, and compressibility have been made. Calculations have also been made for the complex dynamic local field $G(k,\omega)$ for arbitrary values of wave number and frequency. Comparison has been made with the available experimental data for Al ($r_s=2.0$). A critique of the theory is presented.

I. INTRODUCTION

This paper is the second in a series devoted to the study of dynamical correlations in an electron liquid at metallic densities. In an earlier paper,[1] hereafter referred to as I, we used the formalism of many-body perturbation theory to evaluate the proper polarizability Q to first order in the interparticle potential. Our calculation was performed for arbitrary wave vector q and frequency ω and thus generalized to the dynamic case the static ($\omega=0$) results obtained earlier by Geldart and Taylor.[2] Having determined Q to first order, a variety of static and dynamic properties of the electron liquid were calculated. It was found that the dynamic structure factor predicted by the theory for Al agreed in its broad features with the experimental measurements of Batson *et al.*,[3] particularly for wave vectors $q \gtrsim k_F$. Static properties like the structure factor $S(q)$ and pair correlation function $g(r)$ were also found to be significantly improved over their values in the random-phase approximation (RPA).

A major shortcoming of the first-order theory is its inability to produce a finite width for the long-wavelength plasmon. Also, the high-frequency tail in the experimentally measured dynamic structure factor cannot be accounted for. Both these effects arise from multiparticle excitations which lie outside the scope of this approximation. If we attempt to include these effects in our treatment by going to higher order in perturbation, we are immediately faced with a number of difficulties. It has already been mentioned in I that the first-order theory breaks down in the vicinity of the characteristic frequencies $\omega_s=(\hbar/2m)|q^2\pm 2qk_F|$, since Q becomes singular there. Also the perturbation series for Q contains terms in second and higher order which diverge because of the bare Coulomb potential. Although both types of divergences may be eliminated in principle by summing to all orders certain classes of diagrams in the perturbation series (cf. the discussion in I, Secs. IV and V), such a procedure does not seem practically feasible. We therefore conclude that perturbation theory, beyond the first order, is ill suited as a tool for furthering our understanding of the electron dynamics.

A completely different approach to the problem of dynamical correlations is provided by the kinetic-equation method, which has been recently applied to the electron gas problem by Niklasson.[4] In this approach one focuses attention on the Wigner distribution functions of the system and writes down the exact quantum-mechanical equations of motion satisfied by them. The set of coupled equations obtained in this way is the quantum analog of the classical Bogoliubov-Born-Green-Kirkwood-Yvon (BBGKY) hierarchy. Whereas the RPA and other mean-field theories restrict themselves to the first equations of this chain, our

considerations are based on an examination of the second equation in this hierarchy, which describes the motion of two coupled particle-hole excitations. By making a simple, physically motivated truncation of this equation we are led to an expression for the proper polarizability of the form $Q=Q^0+Q^c$, where Q^0 is the Lindhard (RPA) polarizability and Q^c is a correction to it that we have calculated. It turns out that the correction term Q^c has a number of interesting properties: (1) it incorporates explicitly the coupled propagation of two particle-hole pairs, an effect which is absent in the RPA, (2) it has the correct high-frequency behavior required to satisfy the first- and third-frequency-moment sum rules for the spectral response function, which guarantees that the theory has a good short-time behavior, and (3) it contains within it all the first-order diagrams for the proper polarizability discussed in I, as well as a certain class of higher-order diagrams.

Occurring in our expression for Q^c is the equilibrium two-particle Wigner distribution function whose exact form is not known *a priori*. The two simple *Ansätze* that we have tried out for this function are consistent with all the known constraints on it. On evaluating $Q^c(q,\omega)$ in the limit of long wavelength, we find that its real and imaginary parts are proportional to q^2. This leads to a reduction in the plasmon energy from its RPA value and also to a finite width for the long-wavelength plasmon. The microscopic origin of this width is not hard to understand; because of the coupled pair propagation present in Q^c the long-wavelength plasmon can decay into two particle-hole pairs with conservation of both energy and momentum, a channel not open to it in the RPA. Another modification (over RPA and the first-order theory) that occurs at long wavelength is in the compressibility, arising from the extra correlational effects present in Q^c. An evaluation of $Q^c(q\omega)$ for arbitrary q and ω finally provides complete information (within the present model) of the static and dynamic properties of the electron gas.

The organization of this paper is as follows: In Sec. II we outline the formulation of the problem in the language of quantum kinetic equations. In Sec. III we introduce the basic approximation of our theory and use it to obtain an expression for the proper polarizability. In Sec. IV we show how the first-order perturbation theory of I can be recovered as a limiting case of the present work; we also propose two approximate representations of the equilibrium two-particle Wigner function. In Sec. V we specialize our theory to the limit of long wavelength and calculate the dispersion and damping of the plasmon as a function of wave vector. Our results are compared with experiment for the free-electron-like metals Al and Na. In Sec. VI we evaluate our proper polarizability for arbitrary wave vectors and examine its broad features. In Sec. VII we obtain an expression for the complex, frequency-dependent local field $G(q,\omega)$. The static part of our local field is compared with that of Geldart and Taylor[2] and the two are found to agree well at both small and large wave vectors. In Sec. VIII we calculate the compressibility and find that the compressibility sum rule is remarkably well satisfied at $r_s=2.0$; for $r_s=4.0$, however, the situation is less promising. In Sec. IX we explore further the significance of our basic approximation. In Sec. X we calculate the energy-loss function $\mathrm{Im}[-1/\epsilon(q\omega)]$ and compare it with the detailed line shapes for Al obtained by Batson *et al.*[3] from their electron scattering experiments. Results are also given for sodium ($r_s=4.0$). Finally, in Sec. XI we conclude by making a critical assessment of our theory in the light of its overall comparison with experiment.

II. MICROSCOPIC FORMULATION OF THE PROBLEM

We consider a system of N electrons contained in a box of volume V together with a static uniform background of positive charge. The second quantized Hamiltonian for the system in the presence of a weak external potential Φ^{ext} is

$$H=\sum_{\vec{k}\sigma}\frac{\hbar^2k^2}{2m}a^{\dagger}_{\vec{k}\sigma}a_{\vec{k}\sigma}+\frac{1}{2V}{\sum_{\vec{q}}}'v(\vec{q})\sum_{\vec{k}\sigma}\sum_{\vec{k}'\sigma'}a^{\dagger}_{\vec{k}-(\vec{q}/2)\sigma}a^{\dagger}_{\vec{k}'+(q/2)\sigma'}a_{\vec{k}'-(\vec{q}/2)\sigma'}a_{\vec{k}+(\vec{q}/2)\sigma}$$

$$+\frac{1}{V}\sum_{\vec{q}}\Phi^{\mathrm{ext}}(-\vec{q},t)\sum_{\vec{k}\sigma}a^{\dagger}_{\vec{k}-(\vec{q}/2)\sigma}a_{\vec{k}+(\vec{q}/2)\sigma},\quad v(q)=4\pi e^2/q^2\,, \tag{2.1}$$

where $a^{\dagger}_{\vec{k}\sigma}$ and $a_{\vec{k}\sigma}$ are the creation and destruction operators for an electron of momentum $\vec{k}$ and spin σ. The prime on the second term denotes the omission of $\vec{q}=0$ from the summation; this bit is canceled out by the uniform positive background. We shall restrict our considerations to $T=0$. Also, we shall work in Fourier $(\vec{q},\omega)$ space, where $\vec{q}$ and ω represent, respectively, the wave vector and the frequency of a single Fourier component of the external potential $\Phi^{\text{ext}}(\vec{r},t)$ which drives the system out of equilibrium.

The one-particle Wigner function is defined as

$$f^{(1)}_{\vec{k}\sigma}(\vec{q},t)=\langle a^{\dagger}_{\vec{k}-(\vec{q}/2)\sigma}(t)a_{\vec{k}+(\vec{q}/2)\sigma}(t)\rangle \ , \quad (2.2)$$

where the expectation value is taken in the exact ground state of the many-particle system. The electron density is given by

$$n(q)=\sum_{\vec{k}\sigma} f^{(1)}_{\vec{k}\sigma}(q\omega) \ . \quad (2.3)$$

The two-particle Wigner function is defined as

$$f^{(2)}_{\vec{k}\sigma,\vec{k}'\sigma'}(\vec{q},\vec{q}',t)=\langle a^{\dagger}_{\vec{k}-(\vec{q}/2)\sigma}(t)a^{\dagger}_{\vec{k}-(\vec{q}'/2)\sigma'}(t)a_{\vec{k}'+(\vec{q}'/2)\sigma'}(t)a_{\vec{k}+(\vec{q}/2)\sigma}(t)\rangle - f^{(1)}_{\vec{k}\sigma}(\vec{q},t)f^{(1)}_{\vec{k}'\sigma'}(\vec{q}',t) \ . \quad (2.4)$$

Notice that the uncorrelated part has been separated out on the right so that $f^{(2)}$ is the totally correlated part of the two-particle Wigner function. Using the Hamiltonian (2.1) and the usual anticommutation rules for the fermion operators a, $a^{\dagger}$ one obtains the following linearized equation of motion for the one-particle Wigner function:

$$\left[\hbar\omega+i\eta-\frac{\hbar^2}{m}\vec{k}\cdot\vec{q}\right]\bar{f}^{(1)}_{\vec{k}\sigma}(\vec{q}\omega)=\frac{1}{V}(n_{\vec{k}-(\vec{q}/2)\sigma}-n_{\vec{k}+(\vec{q}/2)\sigma})[\Phi^{\text{ext}}(\vec{q}\omega)+v(\vec{q})\bar{n}(\vec{q}\omega)]$$

$$+\frac{1}{V}\sum_{\vec{q}'}v(\vec{q}')\sum_{\vec{k}'\sigma'}[\bar{f}^{(2)}_{\vec{k}-(\vec{q}'/2)\sigma,\vec{k}'\sigma'}(\vec{q}-\vec{q}',\vec{q}',\omega)-\bar{f}^{(2)}_{\vec{k}+(\vec{q}/2)\sigma,\vec{k}'\sigma'}(\vec{q}-\vec{q}',\vec{q}',\omega)] \ . \quad (2.5)$$

Note the following: (1) in the above equation a bar over any quantity indicates that it is the deviation of that quantity from its equilibrium value in the absence of the external potential, e.g., $\bar{n}$ is the change in the density from the homogeneous equilibrium value $n=N/V$, (2) the quantity $\eta=0^+$ has been introduced into the flow term on the left to ensure that the system response is casual, and (3) $n_{\vec{k}\sigma}$ is the equilibrium one-particle Wigner function for a gas of *interacting* electrons and not the free-electron Fermi function $n^0_{\vec{k}\sigma}=\theta(k_F-|\vec{k}|)$. If we neglect the last term in Eq. (2.5) and further replace $n_{\vec{k}\sigma}$ by $n^0_{\vec{k}\sigma}$ we recover the random-phase approximation. In order to go beyond the RPA it is necessary to retain, in some average way, the short-range exchange-correlation effects represented by the last term in Eq. (2.5). In an important class of theories,[5,6] this is done by making an *ansatz* for the two-particle distribution function $f^{(2)}$. One then finds that the Hartree mean field is modified by the presence of a local field factor G, which is expressible in terms of the equilibrium pair correlation function. However, the local field so obtained is usually static and is unable to account properly for the dynamical phenomena of interest to us. We shall not attempt to push this approach further, but instead base our treatment on a consideration of the exact equation of motion for the two-particle distribution function $\bar{f}^{(2)}$.

Using the Hamiltonian (2.1), the linearized equation of motion for $\bar{f}^{(2)}$ can be obtained as

$$\left[\hbar\omega+i\eta-\frac{\hbar^2}{m}\vec{k}\cdot\vec{q}+\frac{\hbar^2}{m}\vec{k}'\cdot\vec{q}'\right]\bar{f}^{(2)}_{\vec{k}\sigma,\vec{k}'\sigma'}(\vec{q}\,\vec{q}'\omega)=F^{\text{ext}}_{\vec{k}\sigma,\vec{k}'\sigma'}(\vec{q}\,\vec{q}'\omega)+F^{\text{ext}}_{\vec{k}'\sigma',\vec{k}\sigma}(\vec{q}'\vec{q}\omega)$$

$$+F^{(2)}_{\vec{k}\sigma,\vec{k}'\sigma'}(\vec{q}\,\vec{q}'\omega)+F^{m}_{\vec{k}\sigma,\vec{k}'\sigma'}(\vec{q}\,\vec{q}'\omega)+F^{m}_{\vec{k}'\sigma',\vec{k}\sigma}(\vec{q}'\vec{q}\omega) \ . \quad (2.6)$$

This equation describes the coupled motion of two particle-hole excitations of average momenta k and k'. The expressions for the various terms on the right-hand side and their physical interpretation have been given in Niklasson's paper.[4] Rather than repeat the discussion here, we will only reproduce those expressions that are of relevance to us and comment briefly on their significance. The first of these terms is

$$F^{\rm ext}_{\vec{k}\sigma,\vec{k}'\sigma'}(\vec{q}\,\vec{q}\,'\omega)=\frac{1}{V}[f^{(2)}_{\vec{k}-(\vec{q}+\vec{q}\,'/2)\sigma,\vec{k}'\sigma'}(-\vec{q}\,')-f^{(2)}_{\vec{k}+(\vec{q}+\vec{q}\,'/2)\sigma,\vec{k}'\sigma'}(-\vec{q}\,')]\Phi^{\rm ext}(\vec{q}+\vec{q}\,',\omega)\ . \tag{2.7}$$

Here $f^{(2)}$ is the equilibrium two-particle Wigner function. This term, in a semiclassical interpretation represents the force exerted by the external potetnial on the particle $\vec{k}$ when it is in the presence of the second particle $\vec{k}'$. The term

$$F^{m}_{\vec{k}\sigma,\vec{k}'\sigma'}(\vec{q}\,\vec{q}\,'\omega)=\frac{1}{V}[f^{(2)}_{\vec{k}-(\vec{q}+\vec{q}\,'/2)\sigma,\vec{k}'\sigma'}(-\vec{q}\,')-f^{(2)}_{\vec{k}+(\vec{q}+\vec{q}\,'/2)\sigma,\vec{k}'\sigma'}(-\vec{q}\,')]v(\vec{q}+\vec{q}\,')\bar{n}(\vec{q}+\vec{q}\,',\omega)+\cdots \tag{2.8}$$

describes the force exerted by the rest of the medium on particle $\vec{k}$ when it is in the presence of particle $\vec{k}'$. It consists of a number of parts. The part actually shown has the structure of a screening field which acts to screen the external force term (2.7) shown above. The remaining parts, indicated by dots, include other screening fields (which act on $F^{(2)}$) and also a contribution arising from the correlated motion of three particle-hole pairs. The two-body term $F^{(2)}$, which has not been displayed explicitly here, represents the mutual force exerted by the particle $\vec{k}$ and $\vec{k}'$ on each other. It should be noted that Eq. (2.6) is symmetric in the excitations $\vec{k}$ and $\vec{k}'$, i.e., it remains invariant under the interchange $(\vec{k}\sigma\vec{q})\rightleftarrows(\vec{k}'\sigma'\vec{q}')$.

III. GENERALIZED RANDOM-PHASE APPROXIMATION

We now truncate Eq. (2.6) in the following way: On the right-hand side we retain only the forcing terms due to the external potential ($F^{\rm ext}$) and those parts of the medium fields (F^{m}) that go into screening $F^{\rm ext}$. Our approximation for $\bar{f}^{(2)}$ is, therefore,

$$\bar{f}^{(2)}_{\vec{k}\sigma,\vec{k}'\sigma'}(\vec{q}\,\vec{q}\,'\omega)\simeq\frac{1}{V}\frac{1}{\tilde{D}(\vec{k},\vec{k}',\vec{q},\vec{q},')}[f^{(2)}_{\vec{k}-(\vec{q}+\vec{q}\,'/2)\sigma,\vec{k}'\sigma'}(-\vec{q}\,')-f^{(2)}_{\vec{k}+(\vec{q}+\vec{q}\,'/2)\sigma,\vec{k}'\sigma'}(-\vec{q}\,')]$$
$$\times[\Phi^{\rm ext}(\vec{q}+\vec{q}\,',\omega)+v(\vec{q}+\vec{q}\,')\bar{n}(\vec{q}+\vec{q}\,',\omega)]+\cdots \tag{3.1}$$

where the ellipsis represent the interchange term $(\vec{q}\,\vec{k}\sigma)\rightleftarrows(\vec{q}\,'\vec{k}'\sigma')$ and where

$$\tilde{D}(\vec{k},\vec{k}',\vec{q},\vec{q}\,')=\hbar\omega+i\eta\frac{\hbar^2}{m}\vec{k}\cdot\vec{q}-\frac{\hbar^2}{m}\vec{k}'\cdot\vec{q}\,'\ . \tag{3.2}$$

It is useful here to recall the RPA which, in terms of $\bar{f}^{(1)}$, can be written as

$$\bar{f}^{(1)}_{\vec{k}\sigma}(\vec{q}\omega)\simeq\frac{1}{V}\frac{1}{D(\vec{k},\vec{q})}(n^{0}_{\vec{k}-(\vec{q}/2)\sigma}-n^{0}_{\vec{k}+(\vec{q}/2)\sigma})$$
$$\times[\Phi^{\rm ext}(\vec{q}\omega)+v(\vec{q})\bar{n}(\vec{q}\omega)]\ , \tag{3.3a}$$

where

$$D(\vec{k},\vec{q})=\hbar\omega+i\eta-\frac{\hbar^2}{m}\vec{k}\cdot\vec{q}\ . \tag{3.3b}$$

Equation (3.1) is the direct generalization of (3.3a) to the case of the two-particle equation and we shall, therefore, refer to it in what follows as the generalized random-phase approximation or GRPA. Our motivations in adopting this approximation are the following: (i) its analogy with the familiar RPA, which successfully incorporates the effects of screening at long wavelengths, (ii) its exact compliance with the first- and third-frequency-moment sum rules, which guarantees a good short-time behavior for the theory, and (iii) the simplicity and tractability it brings to an otherwise seemingly impenetrable problem.

In making the GRPA we are neglecting completely the correlated motion of three particle-hole pairs (contained in F^{m}) as well as certain dynamical two-body terms (the whole of $F^{(2)}$ and part of

F^m). The neglect of $F^{(2)}$ particularly is a cause for some worry since it includes the effects of plasmon-plasmon scattering in lowest order and may be as important at metallic densities as some of the terms we have retained. However, in view of the arguments for the GRPA presented above, we feel there is sufficient appeal in it to warrant our pursuing it further. The true merits and defects of this scheme will emerge in the course of our analysis and will be commented on more fully in the sequel.

On substituting (3.1) into (2.5), dividing out by the one-particle flow term on the left, and summing over all $\vec{k}\sigma$ we obtain

$$\bar{n}(\vec{q}\omega)=[\pi^0(\vec{q}\omega)+\pi^c(\vec{q}\omega)] \times[\Phi^{\text{ext}}(\vec{q}\omega)+v(\vec{q})\bar{n}(\vec{q}\omega)] , \tag{3.4}$$

where

$$\pi^0(\vec{q}\omega)=\frac{1}{V}\sum_{\vec{k}\sigma}\frac{n^0_{\vec{k}-(\vec{q}/2)\sigma}-n^0_{\vec{k}+(\vec{q}/2)\sigma}}{D(\vec{k}\vec{q})} \tag{3.5}$$

is the familiar Lindhard function and

$$\pi^c(\vec{q}\omega)=\frac{1}{V^2}\sum_{\vec{q}'}v(\vec{q}')\sum_{\vec{k}\sigma}\left[\frac{1}{D(\vec{k}+(\vec{q}'/2),\vec{q})}-\frac{1}{D(\vec{k}-(\vec{q}'/2),\vec{q})}\right] \times\sum_{\vec{k}'\sigma'}\frac{1}{\tilde{D}(\vec{k},\vec{k}',\vec{q}-\vec{q}',\vec{q}')}[f^{(2)}_{\vec{k}-(\vec{q}'/2)\sigma,\vec{k}'\sigma'}(-\vec{q}')-f^{(2)}_{\vec{k}+(\vec{q}'/2)\sigma,\vec{k}'\sigma'}(-\vec{q}') +f^{(2)}_{\vec{k}'-(\vec{q}'/2)\sigma',\vec{k}\sigma}(-\vec{q}+\vec{q}')-f^{(2)}_{\vec{k}'+(\vec{q}'/2)\sigma',\vec{k}\sigma}(-\vec{q}+\vec{q}')] . \tag{3.6}$$

Thus, in GRPA the electrons respond to the Hartree potential as in RPA, but with the modified proper polarizability $\pi^0+\pi^c$. The post-RPA effects are contained in the term π^c. Alternatively, we can recast (3.4) in the form

$$\bar{n}(\vec{q}\omega)=\pi^0(\vec{q}\omega)\{\Phi^{\text{ext}}(\vec{q}\omega) +v(\vec{q})[1-G(\vec{q}\omega)]\bar{n}(\vec{q}\omega)\} ,$$

which defines the dynamic local-field factor $G(\vec{q}\omega)$. In GRPA we find

$$G(\vec{q}\omega)=\frac{1}{Q^0(\vec{q}\omega)}-\frac{1}{Q^0(\vec{q}\omega)+Q^c(\vec{q}\omega)} ,$$

where

$$Q^{0,c}(\vec{q}\omega)=-v(\vec{q})\pi^{0,c}(\vec{q}\omega) .$$

According to this second interpretation, the electrons respond as *free* particles to the Hartree mean field modified by the dynamic local field $G(\vec{q}\omega)$. Of the two interpretations we have given, the first is more in line with perturbation theory, in which one expresses the proper polarizability as a sum of terms involving increasing powers of the potential, while the second is more closely allied with approaches based on the approximate decoupling of the kinetic equations.

The structure of the term π^c merits some comment: Of the wave vectors entering it, $\vec{q}$ is associated with the external momentum transfer, $\vec{k}$ with a particle in the system and $\vec{k}'$ with a particle in the correlation hole of $\vec{k}$. The denominators $\tilde{D}$ and the equilibrium Wigner functions $f^{(2)}$ couple the motions of the particle $\vec{k}$ and $\vec{k}'$. It is this latter feature which gives rise to many of the interesting effects in GRPA, as we shall see below.

In order to make contact with earlier work we now introduce an alternative truncation of Eq. (2.6) that is closely related to our GRPA. In this scheme, one retains only the forcing terms due to the external potential, i.e., in Eq. (3.1) the term $v\bar{n}$ is omitted throughout. Since this is a direct generalization of the ordinary Hartree-Fock approximation on the one-particle kinetic equation [Eq. (3.3) with $v\bar{n}$ omitted], we will refer to it as GHFA. By contrasting GHFA with GRPA below, we shall highlight the significance of the additional screening fields which the latter contains.

In the limit of large $\vec{q}$ or ω the distinction between GRPA and GHFA disappears and, in fact, both approximations become formally exact. The reason for this is the following: At short distances or times, the particles do not interact appreciably with each other and respond only to the external potential F^{ext}; the screening fields retained in GRPA thus do not come into play. If the energy denominators D and $\tilde{D}$ in π^c are expanded in inverse powers of $[\hbar\omega\pm(\hbar^2q^2/2m)]$, with only leading terms being retained, then both GHFA and GRPA lead to exactly the expressions for the local field

$G(q\omega)$ first obtained by Niklasson (see Ref. 4). We note in passing that Niklasson's local field, although frequency dependent, is purely real. It should also be emphasized that Niklasson's local field applies only at large q or ω but that it is *exact* in either of these limits.

When we imply in the previous paragraph that GHFA and GRPA become exact at large ω, what we mean is that both schemes satisfy exactly the first- and third-frequency-moment sum rules. This follows from the following asymptotic property of Q^c:

$$\lim_{\omega\to\infty}\left[\frac{\omega^4}{\omega_P^4}Q^c(\vec{q}\omega)\right]=G^{\mathrm{PV}}(q)\ , \tag{3.10}$$

where the definition of $G^{\mathrm{PV}}(q)$ and discussion of the moment sum rules may be found in Sec. III of I.

IV. CONNECTION OF THE PRESENT APPROACH WITH PERTURBATION THEORY; APPROXIMATIONS FOR $f^{(2)}$

Equation (3.6) for π^c contains the equilibrium two-particle Wigner function $f^{(2)}$ which is not known as an explicit function of its arguments. We shall now investigate the consequences of approximating $f^{(2)}$ by the expression

$$f^{(2)\mathrm{HF}}_{\vec{k}\sigma,\vec{k}'\sigma'}(\vec{q})=-\delta_{\vec{k}\vec{k}'}\delta\sigma\sigma' n^0_{\vec{k}+(\vec{q}/2)\sigma}n^0_{\vec{k}-(\vec{q}/2)\sigma}\ , \tag{4.1}$$

which is obtained by evaluating (2.4) with the noninteracting ground-state wave function of the system. It is easily verified that $f^{(2)\mathrm{HF}}$ satisfies the relation

$$\frac{1}{N}\sum_{\vec{k}\sigma;\vec{k}'\sigma'} f^{(2)\mathrm{HF}}_{\vec{k}\sigma,\vec{k}'\sigma'}(\vec{q})=S^{\mathrm{HF}}(\vec{q})-1\ , \tag{4.2}$$

where $S^{\mathrm{HF}}(q)$ is the Hartree-Fock structure factor. On substituting (4.1) into (3.6) and simplifying the resulting expression we find

$$\pi^c_{\mathrm{HF}}(\vec{q}\omega)=\pi^{\mathrm{SE}}(\vec{q}\omega)+\pi^{\mathrm{Ex}}(\vec{q}\omega)\ , \tag{4.3}$$

where the expressions for $\pi^{\mathrm{SE}}(\vec{q}\omega)$ and $\pi^{\mathrm{Ex}}(\vec{q}\omega)$ are given in Eqs. (2.7) and (2.8) of I. Thus π^c_{HF} is simply the sum of the first-order self-energy and exchange graphs in the perturbation expansion of the proper polarizability. This demonstrates that the first-order result of I is contained in the present theory as a special case. Although we cannot extract the higher-order diagrams present in π^c (since $f^{(2)}$ is unknown), we can clarify the situation by going to the $\omega\to\infty$ limit, in which case π^c is known exactly from the third moment [see Eq. (3.10) above and Sec. III of I]. Since π^c in this limit is expressed in terms of $S(q)$, which is a nonanalytic function of r_s, it must therefore contain an infinite subset of diagrams in the perturbation series.

In order to extract more than just the first-order diagrams from π^c we must use in place of (4.1) a more sophisticated approximtion for $f^{(2)}$. A straightforward method of proceeding would be to make a perturbation expansion for $f^{(2)}$ in powers of the potential. However, a more fruitful approach seems to be to try and express $f^{(2)}$ approximately in terms of the static structure factor $S(q)$. Since the latter quantity contains the potential implicitly to all orders, one hopes thereby to have simulated the effect of a large number of terms in the perturbation expansion. In choosing an approximate representation for $f^{(2)}$ in terms of S, one is constrained by the following exact relation connecting the two:

$$S(\vec{q})-1=\frac{1}{N}\sum_{\vec{k}\sigma}\sum_{\vec{k}'\sigma} f^{(2)}_{\vec{k}\sigma,\vec{k}'\sigma'}(\vec{q})\ , \tag{4.4}$$

which follows from the definition of the structure factor. [Note that Eq. (4.2) is a special case of (4.4)].

We now propose the following two approximations for $f^{(2)}$:

Ansatz A:

$$f^{(2)A}_{\vec{k}\sigma,\vec{k}'\sigma'}(\vec{q})=f^{(2)\mathrm{HF}}_{\vec{k}\sigma,\vec{k}'\sigma'}(\vec{q})+\frac{1}{N}n^0_{\vec{k}\sigma}n^0_{\vec{k}'\sigma'}[S(\vec{q})-S^{\mathrm{HF}}(\vec{q})]. \tag{4.5}$$

Ansatz B:

$$f^{(2)B}_{\vec{k}\sigma,\vec{k}'\sigma'}(\vec{q})=f^{(2)\mathrm{HF}}_{\vec{k}\sigma,\vec{k}'\sigma'}(\vec{q})+\frac{1}{2N}(n^0_{\vec{k}-(\vec{q}/2)\sigma}n^0_{\vec{k}'+(\vec{q}/2)\sigma'}+n^0_{\vec{k}+(\vec{q}/2)\sigma}n^0_{\vec{k}'-(\vec{q}/2)\sigma'})[S(\vec{q})-S^{\mathrm{HF}}(\vec{q})]\ , \tag{4.6}$$

where $f^{(2)\mathrm{HF}}_{\vec{k}\sigma,\vec{k}'\sigma'}(q)$ has been defined earlier in (4.1). It is easily verified that both (4.5) and (4.6) are consistent with the relation (4.4). The structure of both (4.5) and (4.5) is such that the zeroth order or Hartree-Fock part has been separated out and an *Ansatz* is made on the remaining part containing potential effects. The structure of the *Ansätze* may be clarified still further by examining them in the classical limit, i.e., $\hbar\to 0$, $\hbar\vec{k}\to\vec{p}$ (finite), $n^0_{k\sigma}\to f^0(p)$ (the Maxwellian distribution). Realizing that exchange effects vanish in this limit, one finds easily that both (4.5) and (4.6) reduce to

$$f^{(2)A,B}_{\vec{k}0,\vec{k}'0'}(\vec{q}\,')\to f^{(2)}_{\vec{p},\vec{p}'}(\vec{q})=f^0(\vec{p})f^0(\vec{p}\,')[S(q)-1]\ , \tag{4.7}$$

which will be recognized immediately as being the *exact* representation of the classical two-particle distribution function, $S(q)$ now being the Fourier transform of the classical pair correlation function. Thus, both the *Ansätze* are seen to reduce correctly to the known limiting form in the classical case. While *Ansatz A* is relatively straightforward, *Ansatz B* is a little more complex because it involves a mixing of correlations in position and momentum space. In the remainder of the text we shall quote only formulas obtained on the basis of *Ansatz A*, since we find that it leads to much better results than *Ansatz B*. Formulas pertaining to *Ansatz B* which are long and tedious are given in Ref. 7.

V. DISPERSION AND DAMPING OF THE LONG-WAVELENGTH PLASMON

The energy and linewidth of the long-wavelength plasmon is determined by the complex zeros of the complex dielectric function, i.e.,

$$\epsilon(\vec{q},\omega)=1+Q^0(\vec{q},\omega)+Q^c(\vec{q},\omega)=0\ . \tag{5.1}$$

In the limit $q\to 0$ the above equation yields for the plasmon energy $\omega_{\mathrm{pl}}(q)$ the expression

$$\omega_{\mathrm{pl}}(q)=\omega_p+\tilde{\alpha}q^2-i\Gamma q^2+O(q^4)\ , \tag{5.2}$$

where

$$\tilde{\alpha}=\tilde{\alpha}_{\mathrm{RPA}}\left[1-\frac{5\omega_p^2}{3}\lim_{q\to 0}\left[\frac{\mathrm{Re}Q^c(q,\omega_p)}{q^2}\right]\right]\ ,$$

$$\tilde{\alpha}_{\mathrm{RPA}}=\frac{3}{10\omega_b}\ , \tag{5.3}$$

and for the plasmon width the expression

$$\Gamma=\frac{\omega_p}{2}\lim_{q\to 0}\left[\frac{\mathrm{Im}Q^c(q,\omega_p)}{q^2}\right]\ . \tag{5.4}$$

As in I, we express the wave vector in units of k_F and frequency in units of $2E_f/\hbar$. The plasmon frequency in these units is $\omega_p=(4/9\pi)^{2/3}(3r_s)^{1/2}$.

In order to obtain $\tilde{\alpha}$ and Γ from our theory we need, therefore, to calculate the q^2 coefficient of Q^c. The detailed calculation of the quantity, which makes use of the *Ansätze A* and *B* introduced in the preceding section, has been discussed in Ref. 7 and we shall quote only the final results here. We find, for small q,

$$Q^c(q\omega)=\frac{2}{5}\left[\frac{\omega_p}{\omega}\right]^4\bar{\gamma}(\omega)q^2+O(q^4)\ , \tag{5.5}$$

where

$$\bar{\gamma}(\omega)=\tfrac{3}{8}-\tfrac{3}{256}\int_0^\infty dq'[S(q')-1]H\left[\frac{\omega}{q'}\right]\ . \tag{5.6}$$

For *Ansatz A* we have

$$\begin{aligned}\mathrm{Re}H(\nu)&=R_0(\nu)+R_1(\nu)\ln|\nu+2|\\&\quad+R_2(\nu)\ln|\nu-2|+R_3(\nu)\ln|\nu|\\ \mathrm{Im}H(\nu)&=\pi R_2(\nu)\theta(2-\nu)\ .\end{aligned} \tag{5.7}$$

The functions R_l are defined as follows:

$$\begin{aligned}R_0(\nu)&=16(20-8\nu^2-7\nu^4)\ ,\\ R_1(\nu)&=4(-16\nu+40\nu^3+46\nu^4-7\nu^6)\ ,\\ R_2(\nu)&=4(16\nu-40\nu^3+46\nu^4-7\nu^6)\ ,\\ R_3(\nu)&=-R_1(\nu)-R_2(\nu)\ .\end{aligned} \tag{5.7b}$$

In terms of the function $\bar{\gamma}$, dispersion and damping coefficients are, respectively, given by

$$\tilde{\alpha}=\tilde{\alpha}_{\mathrm{RPA}}\left[1-\frac{2\omega_p^2}{3}\mathrm{Re}\bar{\gamma}(\omega_p)\right]\ , \tag{5.8}$$

$$\Gamma=\frac{\omega_p}{5}\mathrm{Im}\bar{\gamma}(\omega_p)\ . \tag{5.9}$$

Note that the contribution to $\tilde{\alpha}$ from the first-order diagrams [equal to $-\tilde{\alpha}_{\mathrm{RPA}}(2\omega_p^2/3)(3/8)$] together with the remaining correlation contribution opposes the Hartree mean field and leads to a reduction in the plasmon energy from its RPA value. As regards the width, the entire contribu-

tion arises from the post-RPA collisional effects present in Q^c.

The result for the plasmon energy as a function of wave vector, Eq. (5.2), can be recast in a form which is instructive. We write

$$\omega_{\rm pl}(q)=\omega_{\rm RPA}(q)+\Delta E(q,\omega_p) -i\Delta W(q,\omega_p)+O(q^4)\,, \tag{5.10}$$

where

$$\omega_{\rm RPA}(q)=\omega_p+\tilde{\alpha}_{\rm RPA}q^2\,, \tag{5.11a}$$

$$\Delta E(q,\omega)=-\frac{\omega_p}{2}{\rm Re}Q^c(q,\omega)\,, \tag{5.11b}$$

$$\Delta W(q,\omega)=\frac{\omega_p}{2}{\rm Im}Q^c(q,\omega)\,. \tag{5.11c}$$

The first term on the right-hand side of Eq. (5.10) is the plasmon energy in the RPA. When higher-order correlation effects are taken into account, the RPA plasmon is "renormalized" in two ways—it suffers a downward shift ΔE in its energy and at the same time it develops a finite width ΔW. These two quantities are not independent of each other. From the analyticity properties of the complex function Q^c we can establish the following dispersion relation connecting ΔE and ΔW:

$$\Delta E(q,\omega)=\frac{1}{\pi}\mathscr{P}\int_{-\infty}^{\infty}\frac{\Delta W(q,\omega')}{\omega-\omega'}d\omega'\,. \tag{5.12}$$

This relation is perfectly general since the only property used in its derivation was the analyticity of Q^c, which is determined unambiguously by casuality. Relations similar to (5.12) are common in other parts of many-body physics.[8] The point of our mentioning the relation (5.12) is to emphasize that, even in an approximate theory, the plasmon dispersion and damping cannot be independent of each other but must be related through casuality. We have exploited this fact to cut down considerably on the labor leading to our results (5.5)–(5.7). Rather than calculate the dispersion and damping separately, we calculated only the dispersion ΔE and inferred the damping ΔW through analytic continuation in the frequency variable (see Ref. 7 for details).

Before we can obtain numerical results for plasmon dispersion and damping we must evaluate the functions Re and Im$\bar{\gamma}(\omega)$, which are essentially the q^2 coefficients of Re and ImQ^c at small q. To perform the integrals in $\bar{\gamma}(\omega)$ we have used the self-consistent $S(q)$ of Vashishta and Singwi (VS),[6] although it turns out that the result does not depend too sensitively on the particular $S(q)$ used. In Fig. 1(a) we have plotted Re and Im $\bar{\gamma}$, calculated using both *Ansätze A* and *B*, as a function of ω for $r_s=2$ (Al). In Fig. 1(b) we have shown the same functions for $r_s=4$ (Na). The arrows in all figures denote the position of the plasmon frequen-

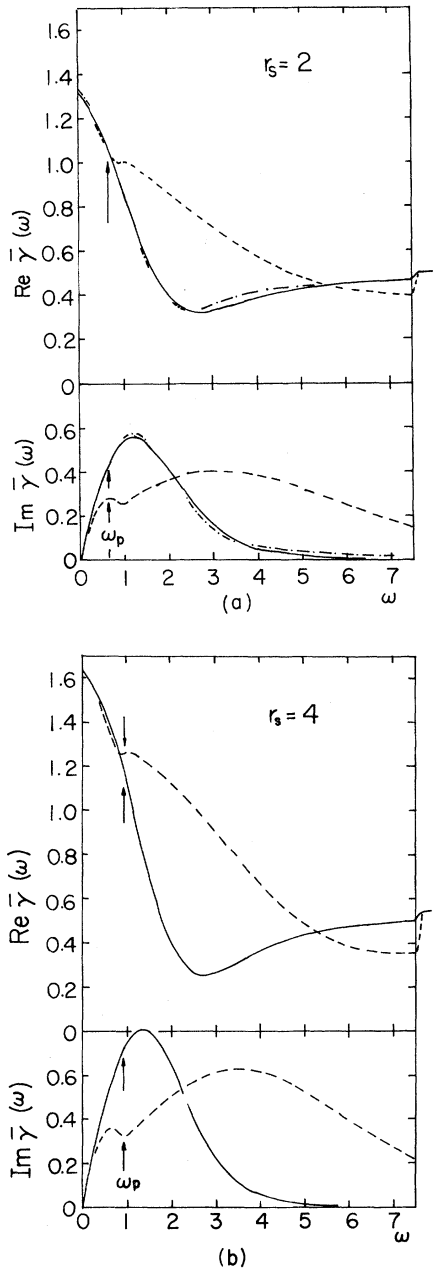

FIG. 1. Function $\bar{\gamma}(\omega)$ vs ω in units of $2E_F/\hbar$, for (a) $r_s=2.0$ (Al) and (b) $r_s=4.0$ (Na). The full (broken) lines represent the results obtained with *Ansatz A* (*Ansatz B*) and the $S(q)$ of VS.[6]

TABLE I. Coefficients of plasmon dispersion $\tilde{\alpha}$ and damping Γ.

Element	Al		Na	
r_s	2.0		4.0	
Ansatz	*A*	*B*	*A*	*B*
ω_p	0.665		0.941	
$\tilde{\alpha}_{\mathrm{RPA}}$	0.451		0.319	
$\mathrm{Re}\bar{\gamma}(\omega_p)$	1.063	1.053	1.154	1.253
$\tilde{\alpha}=\tilde{\alpha}_{\mathrm{RPA}}[1-\frac{2}{3}\omega_p^2\mathrm{Re}\bar{\gamma}(\omega_p)]$	0.310	0.311	0.102	0.083
$\tilde{\alpha}$ Expt.	0.39, Ref. 3		0.24, Ref. 9	
$\mathrm{Im}\bar{\gamma}(\omega_p)$	0.449	0.282	0.725	0.322
Γ/ω_p	0.090	0.056	0.145	0.064
(Γ/ω_p) Expt.	0.13, Ref. 9		0.07, Ref. 9	

cy ω_p; from Eqs. (5.8) and (5.9) we see that the dispersion and damping coefficients are determined by the values of Re and Im$\bar{\gamma}$ at this single point.

Our detailed numerical results for the plasmon dispersion and damping coefficients are shown in Table I together with the RPA predictions and the experimentally measured values of these quantities.[3,9] We see that our predictions $\tilde{\alpha}_{A,B}$ for the dispersion coefficient are somewhat below the experimental values for both Al and Na. On the other hand, the RPA values are seen to be too high. Apparently, the higher-order correlations entering in our theory have the effect of pulling down the RPA dispersion by more than the required amount. The situation is worse for Na than it is for Al.

Equation (5.8) shows that the correction to the RPA dispersion is proportional to $\omega_p^2 \sim r_s$; consequently, any error in estimating it is considerably magnified in the case of Na for which $r_s=4.0$. Our predictions for the relative plasmon width Γ/ω_p are generally less than the experimental values. For Al, the theoretical width is a factor of ~ 2 smaller than experiment while for Na the difference is less. There exist in the literature a number of microscopic calculations of plasmon width at long wavelengths.[10–12] The first attempt was made by DuBois[10] who developed a "golden-rule" formula for the width, applicable at very high densities. This approach was subsequently modified by DuBois and Kivelson[11] and, independently, by Hasegawa and Watabe[12] who included the effects of dynamical screening in the calculation. With this modification it was found that the calculated width was substantially below the experimental value.[13] The contribution of various solid state effects to the plasmon width was studied in a later paper by Hasegawa.[14] All these calculations were perturbative in that they involved expansions in powers of the coupling parameter r_s. Since $r_s \gtrsim 2$ for metals, the validity of such an expansion is uncertain. Our calculation of plasmon width is not perturbative in the sense that the potential enters to all orders through the structure factor $S(q)$ that occurs in our expressions. We have thus included, in an approximation way, the effect of a large number of terms in the perturbation expansion. We feel that our calculation complements the work of earlier authors because, first, it is nonperturbative and, second, it illuminates from a different point of view the role of two-pair excitations in determining the finite width of the long-wavelength plasmon.

VI. EVALUATION OF $Q^c(q)$ AT FINITE q

On evaluating the expression for Q^c, using *Ansatz A*, we find

$$Q^c(\vec{q}\omega)=Q^1(\vec{q}\omega)+Q^h(\vec{q}\omega)\,, \tag{6.1}$$

where Q^1 is the first-order proper polarizability and Q^h is the contribution coming from higher-order potential effects. The explicit form of Q^h is

$$Q^h(\vec{q}\omega)=-\frac{3(\alpha r_s)^2}{4\pi^4 q^3}\int_0^\infty dq'\int_{-1}^{+1}d\mu'$$
$$\times\left\{[S(q')-S_{\rm HF}(q')]\left[\psi\left[\frac{q^2-qq'\mu'}{2},\frac{q^2+qq'\mu'}{2}\right]-\psi\left[\frac{q^2-qq'\mu'}{2},\frac{q^2-qq'\mu'}{2}\right]\right.\right.$$
$$\left.-\psi\left[\frac{qq'\mu'-q^2}{2},\frac{qq'\mu'-q^2}{2}\right]+\psi\left[\frac{qq'\mu'-q^2}{2},\frac{-q^2-qq'\mu'}{2}\right]\right]$$
$$+[S((q^2+q'^2-2qq'\mu')^{1/2})-S_{\rm HF}((q^2+q'^2-2qq'\mu')^{1/2})]$$
$$\left.\times\left[\psi\left[\frac{qq'\mu'}{2},\frac{qq'\mu'}{2}\right]-\psi\left[\frac{qq'\mu'}{2},\frac{-qq'\mu'}{2}\right]-\psi\left[\frac{-qq'\mu'}{2},\frac{qq'\mu'}{2}\right]+\psi\left[\frac{-qq'\mu'}{2},\frac{-qq'\mu'}{2}\right]\right]\right\}, \tag{6.2}$$

where

$$\psi(\omega,\vec{q},\vec{q}\,',H_1,H_2)=\int_{|\vec{k}|\le 1}d^3k'\int_{|\vec{k}|\le 1}d^3k[\omega+i\eta-H_1-\vec{q}\,'\cdot\vec{k}\,'-(\vec{q}-\vec{q}\,')\cdot\vec{k}]^{-1}(\omega+i\eta-H_2-\vec{q}\cdot\vec{k})^{-1} \tag{6.3}$$

To save writing in formula (6.2), we have suppressed the first three arguments of ψ, which are always ω, $\vec{q}$, and $\vec{q}\,'$, and showed only the last two. The imaginary part of ψ turns out to be easier to evaluate than its real part and can, in fact, be expressed entirely in terms of elementary functions. The details of this calculation are described in Ref. 7, and we quote only the final results here:

$$\mathrm{Im}\psi(H_1,H_2)=-\frac{4\pi^3(\vec{q}-\vec{q}\,')^2}{s^2qq'^3}\left[G\left[\frac{\omega-H_1+q'}{|\vec{q}-\vec{q}\,'|}\right]-G\left[\frac{\omega-H_1-q'}{|\vec{q}-\vec{q}\,'|}\right]\right], \tag{6.4a}$$

$$G(x)=G_1(x)+G_2(x), \tag{6.4b}$$

where

$$G_1(x)=\begin{cases}\widetilde{G}_1(1)+\widetilde{F}_1(1)[\frac{1}{2}(x^2-1)-h_0(x-1)] & \text{for } 1<x\\ \widetilde{G}_1(x) & \text{for } -1\le x\le 1\\ \widetilde{G}_1(-1)+\widetilde{F}_1(-1)[\frac{1}{2}(x^2-1)-h_0(x+1)] & \text{for } x<-1,\end{cases} \tag{6.4c}$$

$$\widetilde{G}_1(x)=-\frac{h_0h_2}{2}x^2+\tfrac{1}{3}(h_2+\tfrac{1}{2}ch_0)x^3-\tfrac{1}{8}cx^4-\mathrm{sgn}(h_2-cx)D^4\mathrm{Re}L\left[\frac{x-ch_2}{D},\sigma,\frac{ch_2-h_0}{D}\right], \tag{6.4d}$$

$$\widetilde{F}_1(x)=h_2x-\tfrac{1}{2}cx^2-\mathrm{sgn}(h_2-cx)D^2\mathrm{Re}\Lambda\left[\frac{x-ch_2}{D},\sigma\right], \tag{6.4e}$$

$$G_2(x)=\theta(1-h_2^2)\left[\tfrac{1}{2}ch_2h_0x^2-\tfrac{1}{3}(ch_2+\tfrac{1}{2}h_0)x^3+\tfrac{1}{8}x^4-\mathrm{sgn}(x-ch_2)D^4\mathrm{Re}L\left[\frac{x-ch_2}{D},-1,\frac{ch_2-h_0}{D}\right]\right], \tag{6.4f}$$

$$\Lambda(\xi,\sigma)=\tfrac{1}{2}\xi\lambda(\xi,\sigma)+\tfrac{1}{2}\Gamma(\xi,\sigma), \tag{6.4g}$$

$$L(\xi,\sigma,\xi_0)=[\tfrac{1}{16}(-\sigma\xi+2\xi^3)+\tfrac{1}{6}(-2\sigma+\xi^2)\xi_0]\lambda(\xi,\sigma)+[\tfrac{1}{16}(\sigma+4\xi^2)+\tfrac{1}{2}\xi\xi_0]\Gamma(\xi,\sigma), \tag{6.4h}$$

$$\lambda(\xi,\sigma)=(\xi^2+\sigma)^{1/2}, \tag{6.4i}$$

$$\Gamma(\xi,\sigma)=\sigma\ln[\xi+\lambda(\xi,\sigma)], \tag{6.4j}$$

$$h_0=\frac{\omega-H_1}{|\vec{q}-\vec{q}\,'|},\quad h_2=\frac{\omega-H_2}{|\vec{q}|},\quad c=\frac{(\vec{q}-\vec{q}\,')\cdot\vec{q}}{|\vec{q}-\vec{q}\,'||\vec{q}|},\quad s^2=1-c^2,$$
$$D=s(|h_2^2-1|)^{1/2},\quad \sigma=\mathrm{sgn}(h_2^2-1),\quad \xi_0=\frac{ch_2-h_0}{D}. \tag{6.4k}$$

With a suitable choice of the structure factor $S(q)$, $\mathrm{Im}Q^h$ may now be obtained through numerical integration. In our calculations, the $S(q)$ used was the self-consistent $S(q)$ of Vashishta and Singwi (VS).[6] Once $\mathrm{Im}Q^h$ has been computed the corresponding real part may be obtained numerically through the dispersion relation

$$\mathrm{Re}Q^h(\vec{q}\omega)=-\frac{1}{\pi}\mathscr{P}\int_{-\infty}^{\infty}\frac{\mathrm{Im}Q^h(\vec{q}\omega')}{\omega-\omega'}d\omega' , \tag{6.5}$$

which follows from the fact that the function Q^h is analytic in the upper half of the complex ω plane and falls off asymptotically as ω^{-4}.

In Fig. 2 we have shown the polarizabilities Q^0, Q^1, and Q^h as functions of frequency for momentum transfer $q=1.0$ and electron density $r_s=2.0$. The values of the first-order polarizability Q^1 were taken from I. The frequency regions around $\omega_s=|q^2/2\pm q|$ have been deliberately omitted from Q^1, since we know from the discussion in I that the first-order theory becomes invalid there. The function Q^h has been calculated with both *Ansatz A* (solid line) and *Ansatz B* (dash-dot-line).

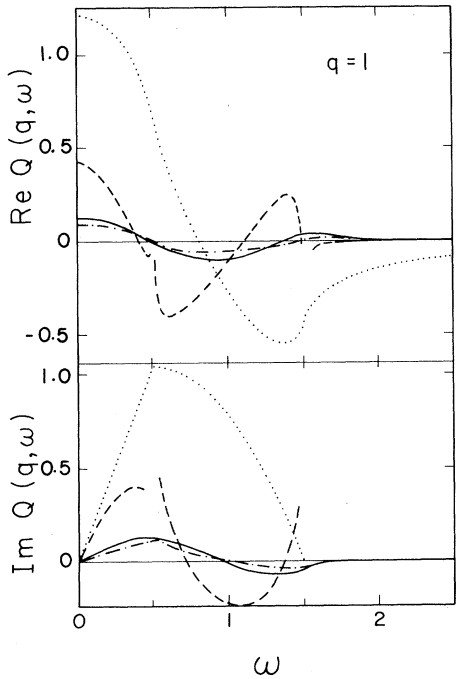

FIG. 2. Proper polarizability at $r_s=2.0$: $\cdots$ $Q^0(q\omega)$; $---$ $Q^1(q\omega)$; — $Q_A^h(q\omega)$; $-\cdot-\cdot-\cdot$ $Q_B^h(q\omega)$. Wave vector q is expressed in units of k_F, frequency ω in units of $2E_F/\hbar$ here and on all other figures.

Where the results for the two *Ansätze* become identical, only the curve for *Ansatz A* has been shown (this convention is followed in all subsequent figures). The first point to note in Fig. 2 is the relative magnitude of the functions Q^0, Q^1, and Q^h: While Q^1 is about 30% of Q^0, Q^h in turn is about 30% of Q^1 or only about 9% of Q^0. Although the absolute magnitude Q^h is small in relation to Q^0 and Q^1, thereby justifying our looking upon it as a correction, the modulation it produces in the total dielectric function $\epsilon=1+Q^0+Q^1+Q^h$ has important consequences, as we shall see later. While both $\mathrm{Im}Q^0$ and $\mathrm{Im}Q^1$ fall off to zero at $w_s=q/2+q$, $\mathrm{Im}Q^h$ has a tail beyond this point. This tail, which is initially negative, causes $S(q\omega)$ to become negative in a narrow frequency region around ω_s (see Sec. X) before it finally becomes positive. The oscillatory character (i.e., the sequence of positive and negative parts) of $\mathrm{Im}Q^h$ ensures that when it is added to $\mathrm{Im}Q(Q^0+Q^1)$ the correct value of the first frequency moment (f sum rule) predicted by RPA and the first-order theory of I is maintained, while the deficiency in the third moment present earlier is made up. For $r_s<2.0$, the magnitude of Q^h becomes negligible compared to Q^1 and we recover substantially all the results of first-order perturbation theory.

On repeating the above calculations for $r_s=4.0$, we found that Q^1 and Q^h were of the order of 70% and 25%, respectively, of the magnitude of Q^0. Thus, at $r_s=4.0$, Q^1 and Q^h are no longer small "corrections" to the RPA, but instead give sizable contributions to the total dielectric functions ϵ. This fact will be recalled later when we discuss the results of our theory at $r_s=4.0$.

VII. THE DYNAMIC LOCAL FIELD

The dynamic local field in the present theory is given by

$$G(\vec{q}\omega)=\frac{1}{Q^0(\vec{q}\omega)}-\frac{1}{Q^0(\vec{q}\omega)+Q^1(\vec{q}\omega)+Q^h(\vec{q}\omega)} . \tag{7.1}$$

In the first-order theory of I, it is given by the above expression with Q^h in the second term omitted. In Fig. 3(a) we have shown the dynamic local fields G (present theory) and G^{Pr} (first-order theory) as functions of frequency for $q=1.0$ and $r_s=2.0$. We see that over most frequencies G_A (solid line) and G_B (dash-dot-line) are qualitatively

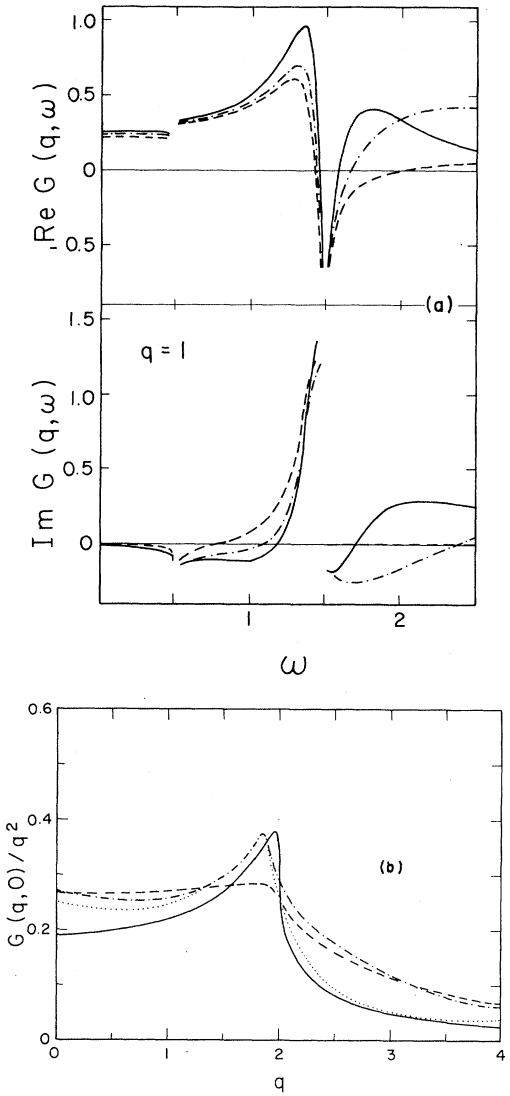

FIG. 3. (a) Dynamic local field at $r_s=2.0$: — — — $G^{Pr}(q\omega)$; — $G_A(q\omega)$; —·—·—·$G_B(q\omega)$. (b) Static part of the local-field function $G(q,0)/q^2$: — G_{Pr}, at $r_s=1.894$; —·—·— G_A at $r_s=2.0$; ··· G_B at $r_s=2.0$; — — — G^{GT}, at $r_s=1.894$.

similar to G^{Pr} (dashed line). However, the difference in the three local fields shows up quite clearly in the frequency region beyond $q^2/2+q$, where $\mathrm{Im}G^{Pr}=0$. For large ω both $\mathrm{Re}G_A$ and $\mathrm{Re}G_B$ tend to the same value G^{PV} $(q=1)=0.16$ dictated by the third moment, while $\mathrm{Re}G^{Pr}$ tends to the value G^{PV}_{HF} $(q=1)=0.11$.

In Fig. 3(b) we have plotted the static part of the local field divided by q^2 as a function of q in (i) the first-order theory of I, (ii) the present theory, both *Ansatz A* and *B*, and (iii) the theory of Geldart and Taylor.[2] It should be pointed out that (i) and (ii) have been calculated at $r_s=1.894$ while (iii) has been calculated at $r_s=2.0$. However, this difference in r_s is small and will be ignored in what follows. The local field of Geldart and Taylor G^{GT} has been adjusted to have the correct value at small q required by the compressibility sum rule. We see that G^{Pr} at $q=0$ lies considerably below G^{GT}, thus implying a large violation of the compressibility sum rule in the first-order theory. However, when the higher-order term Q^h is included, a dramatic improvement results: the local field G_A at $q=0$ is seen to be very close to G^{GT} while G_B is only a little different from it. This shows that the higher-order correlational effects entering in our theory play a crucial role in ensuring the correct compressibility, with *Ansatz A* producing a better result than *Ansatz B*. A detailed quantitative estimate of the compressibility will be presented in the next section.

Returning to the curves for $G(q,0)/q^2$, we see that G^{GT} differs appreciably from the other curves in the vicinity of $q=2$: whereas the other curves exhibit a sharp maximum there, G^{GT} has no such pronounced structure. The sharp maximum present in G^{Pr} is, as we have seen in I, an artifact of the first-order perturbation theory. It is evident that G_A and G_B do not succeed in eliminating this feature and G^{GT} is probably a more accurate representation of the static local field in this region. At very large q our local fields G_A,G_B tend to a common limiting value given by

$$\lim_{q\to\infty} G_{A,B}(q,0)=\tfrac{2}{3}[1-g(0)]\,, \tag{7.2}$$

where $g(0)$ is the pair correlation function at zero separation in our theory. Since $g(0)\geq 0$, $\lim G(q,0)\leq \frac{2}{3}$ in general. For the $S(q)$ of VS, which has been used as input in our calculations, $g(0)=0.033\,22$ and consequently,

$$\lim_{q\to\infty} G_{A,B}(q,0)=0.64\,.$$

It is interesting to note that at the largest q's shown in the figure our local field is practically the same as that of Geldart and Taylor.

VIII. COMPRESSIBILITY

In this section we make a quantitative estimate of the compressibility. In the present theory, the dielectric function is given by

$$\epsilon(\vec{q}\omega)=1+Q^0(\vec{q}\omega)+Q^1(\vec{q}\omega)+Q^h(\vec{q}\omega)\ . \tag{8.1}$$

The limiting forms of the functions Q^0, Q^1, and Q^h at $\omega=0$ and $q\to 0$ are

$$Q^i(\vec{q}0)=\frac{c_i}{q^2}+O(q^0),\quad i=0,1,h \tag{8.2}$$

where

$$c_0=\left[\frac{q_{\rm FT}}{k_F}\right]^2=\frac{4\alpha r_s}{\pi}\ , \tag{8.3a}$$

$$c_1=\frac{4\alpha^2 r_s^2}{\pi^2}\ , \tag{8.3b}$$

and c_h is a quantity (depending only on r_s) which we shall estimate below. On using (8.2) we find in the static, long-wavelength limit

$$\epsilon(\vec{q}0)=\frac{(c_0+c_1+c_h)}{q^2}+O(q^0)\ . \tag{8.4}$$

From Eq. (8.2) we see that c_h may be determined by extrapolation if the function Q^h is known at two (small) values of q. Using the data given in columns 3 and 4 of Table II we obtain for c_h the numbers given in column 5 of the same table. [The accuracy of our extrapolation procedure was checked by calculating the quantities c_0 and c_1 using the same technique and it was found that our estimates differed from the true values (8.3a) and (8.3b) by less than 1%]. In terms of c_i and the compressibility of the noninteracting gas K_f, the compressibility K in the present theory is given by[5]

$$\left[\frac{K_f}{K}\right]_\epsilon=\left[1+\frac{c_1+c_h}{c_0}\right]^{-1}\ . \tag{8.5}$$

The subscript ϵ above indicates that the compressibility has been obtained from the limiting form of the dielectric function. Alternatively, the compressibility may be determined through differentiation of the ground-state energy. In this way one obtains

$$\left[\frac{K_f}{K}\right]_E=1-\frac{4\alpha r_s}{\pi}\left(\tfrac{1}{4}+\gamma_{\rm corr}\right)\ . \tag{8.6}$$

The three terms in the above expression are the contributions arising from the kinetic, exchange, and correlation energies, respectively. For $\gamma_{\rm corr}$ we have taken[11]

$$\gamma_{\rm corr}=(0.0088\pm 0.0008)\ . \tag{8.7}$$

Our calculated values of $(K_f/K)_\epsilon$ are given in the sixth column of Table II and the values of $(K_f/K)_E$ are listed alongside for comparison. We see that for $r_s=2.0$ the compressibility sum rule is remarkably well satisfied, with *Ansatz A* producing a better result than *Ansatz B*. In fact, for *Ansatz A*, the discrepancy between the two estimates is considerably smaller than the magnitude of the correlation-energy contribution to $(K_f/K)_E$. For $r_s=4.0$, our estimate of compressibility is almost twice as large as that obtained from the ground-state energy. The reason for this can perhaps be understood if we recall from Sec. VI that, for $r_s=4.0$, the functions Q^1 and Q^h are fairly appreciable in relation to Q^0. This seems to indicate that the terms we have neglected in our theory may not be small and might compete quite effectively with the terms we have retained in producing the final result. The general conclusion we can draw from this is that owing to the strongness of the correlation term $Q^c=Q^1+Q^h$ and neglecting all other potential effects may not be a very fruitful course at low densities.

IX. COMPARISON BETWEEN GHFA AND GRPA

In this section we compare the two approximation schemes GHFA and GRPA and show that the

TABLE II. Test of the compressibility sum rule.

r_s	*Ansatz*	$Q^h(0.25,0)$	$Q^h(0.50,0)$	C_h	$\left[\frac{K_f}{K}\right]_\epsilon$	$\left[\frac{K_f}{K}\right]_E$
2.0	*A*	4.0741	0.8026	0.2726	0.6505	0.644
	B	2.7890	0.5488	0.1867	0.6792	
4.0	*A*	22.2204	4.4404	1.4817	0.4501	0.243
	B	14.6288	2.9286	0.9750	0.4924	

latter is clearly superior to the former. As we have seen, the only difference between the two is the presence of screening fields in the latter. At first sight it might appear that this difference is not a very significant one. Indeed, it has been shown earlier that in the limit of large q or ω both schemes become identical. However, at lower q and ω the difference between the two schemes is marked, as is evident from the following:

(1) The expression for the density-density response function in GHFA is

$$\chi^{\mathrm{GHFA}}(\vec{q}\omega)=\frac{\pi^0(\vec{q})+\pi^c(\vec{q}\omega)}{1-v(\vec{q})\pi^0(\vec{q}\omega)} . \tag{9.1}$$

Notice that π^c occurs only in the numerator but not in the denominator; this unsymmetrical form makes it impossible to establish a direct connection with perturbation theory. On the other hand, the corresponding expression in GRPA,

$$\chi^{\mathrm{GRPA}}(\vec{q}\omega)=\frac{\pi^0(\vec{q}\omega)+\pi^c(\vec{q}\omega)}{1-v(\vec{q})[\pi^0(\vec{q}\omega)+\pi^c(\vec{q}\omega)]} , \tag{9.2}$$

allows one to establish such a connection very easily.

(2) The dielectric function in GHFA can be shown to be

$$\epsilon^{\mathrm{GHFA}}=1+Q^0+Q^c\frac{(1+Q^0)}{(1-Q^c)} . \tag{9.3}$$

In the limit $q\to 0$, Eq. (9.3) gives for the plasmon energy the expression

$$\omega_{\mathrm{pl}}^{\mathrm{GHFA}}(q)=\omega_p+2\tilde{\alpha}_{\mathrm{RPA}}q^2+O(q^4)+iO(q^4). \tag{9.4}$$

We thus see that in GHFA the plasmon dispersion coefficient is the same as in RPA, the change occurring only in the term of $O(q^4)$. Further, there is no damping of the plasmon to order q^2. On the other hand, GRPA predicts modifications in dispersion and damping of order q^2 (see Sec. V), in line with experiment and also with other theoretical estimates based on perturbation theory.[10–12]

(3) In the static long-wavelength limit the dielectric function in GHFA becomes

$$\epsilon_{q\to 0}^{\mathrm{GHFA}}(\vec{q}0)=-\frac{C_0}{(C_\perp+C_n)}+O(q^2) . \tag{9.5}$$

From this it is evident that ϵ^{GHFA} violates the perfect screening requirement which demands that $\lim_{q\to 0}[(1/\epsilon(\vec{q}0)]=0$. However, in GRPA the dielectric function is consistent with this requirement as is obvious from Eq. (8.4). We can conclude from the above discussion that, as in the case of the one-particle kinetic equation, the inclusion of screening effects in the two-particle equation is a matter of crucial importance.

X. DYNAMIC STRUCTURE FACTOR: COMPARISON WITH EXPERIMENT

The dynamic structure factor $S(q\omega)$ is expressed in terms of the energy-loss function $\mathrm{Im}[-1/e(q\omega)]$ through the relation

$$S(q\omega)=\frac{3q^2}{4\alpha r_s}\mathrm{Im}\left[-\frac{1}{\epsilon(q\omega)}\right] , \tag{10.1}$$

where q is in units of k_F and S in units of $\hbar/2E_F$. The expression for the energy-loss function in the present theory is

$$\mathrm{Im}\left[-\frac{1}{\epsilon(q\omega)}\right]=\mathrm{Im}\left[\frac{-1}{1+Q^0(q\omega)+Q^1(q\omega)+Q^{\hbar}(q\omega)}\right] . \tag{10.2}$$

If Q^h is omitted in Eq. (10.2) we get the expression for the loss function in first-order perturbation theory; if both Q^h and Q^1 are omitted we are back to the RPA. In Fig. 4(a)–4(c), we compare our theoretical calculations of the loss function with the experimentally measured line shapes by Batson *et al.*[3] The theoretical curves shown are (1) RPA (solid line labeled RPA), (2) first-order perturbation theory (dashed line), (3) present theory with *Ansatz A* (solid line labeled *A*), and (4) present theory with *Ansatz B* (dash-dot line). The experimental points are shown by heavy dots in the figures.

We turn first to Fig. 4(a) which shows the loss function at momentum transfer $q=2.0$ Å^{-1} $=1.1412k_F$. We have already remarked in I that in going from the RPA to the first-order theory (FO) the peak position of the loss function shifts downward in energy until it practically coincides with experiment. We observe now that in passing from FO to the present theory the peak position of the loss function shifts downward in energy until it practically coincides with experiment. We also observe that in passing from FO to the present theory the shift in peak position is almost imperceptible but the absolute intensity of the loss function rises until it comes very close to experiment.

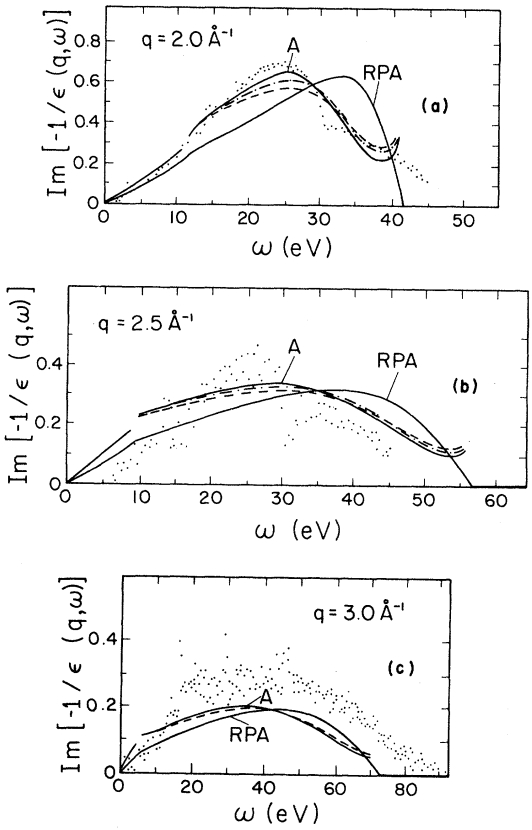

FIG. 4. (a) Energy-loss function $\mathrm{Im}[-1/\epsilon(q\omega)]$ [proportional to $S(q\omega)$] for $q=2.0$ Å^{-1} at $r_s=2.0$; — RPA (labeled); $-\cdot-\cdot-\cdot$ FO, Ref. 1; — present theory with *Ansatz A* (labeled); — — — present theory with *Ansatz B*; experimental points are the measurements of Batson (Ref. 3) for aluminum. Note the units for q and ω used in these figures. (b) Same as 4(a) for $q=2.5$ Å^{-1}. (c) Same as (a) for $q=3.0$ Å^{-1}.

With *Ansatz A*, particularly, we find that we can reproduce quite well the overall line shape of Batson *et al.*

Another new feature of our theory compared to RPA and FO is the appearance of a high-frequency tail in the loss function, although this is too small to be visible in the figure. Two negative aspects of our theory are (1) its failure to remove the singularities at $\omega_s=|(q^2/2)\pm q|$ present in the first-order term Q^1 (because of this, our theory, like FO, becomes invalid in the vicinity of ω_s and we have deliberately not shown results for it there), and (2) the occurrence of a small negative portion in $\mathrm{Im}(-1/\epsilon)$ in the neighborhood of the RPA cutoff $q^2/2+q$. To understand the origin of this negative portion we note from (10.2) that $\mathrm{Im}(-1/\epsilon)\simeq\mathrm{Im}(Q^0+Q^1+Q^h)$. On examining Fig. 2 we see that both $\mathrm{Im}Q^0$ and $\mathrm{Im}Q^1$ fall off sharply to zero at $q^2/2+q$, while $\mathrm{Im}Q^h$ is negative in this region and later develops a positive tail.

It is this behavior of $\mathrm{Im}Q^h$ which is reflected directly in the loss function for $\omega\geq q^2/2+q$. We should mention that the negative portion in $\mathrm{Im}(-1/\epsilon)$ around $q^2/2+q$, like the positive high-frequency tail, is too small to be visible in Figs. 4(a)–4(c). The occurrence of a negative portion in $\mathrm{Im}Q^h$ cannot be regarded as spurious since we know from our discussion of Sec. II that such a piece is necessary in order to keep the f-sum rule intact (the negative part in $\mathrm{Im}Q^1$ occurs for the same reason). What is necessary is that the negative bit in $\mathrm{Im}Q^h$ occur somewhat *below* $q^2/2+q$ so that it can be compensated for by the large and positive $\mathrm{Im}Q^0$. This fine balance is lacking in our theory. If we ignore the frequency regions in the vicinity of $|q^2/2\pm q|$, where we have seen that our theory breaks down, we find that for other frequencies our calculated loss function at $q=2.0$ Å^{-1} agrees remarkably well with the line shape of Batson *et al.*

Figure 4(b) shows the line shape for $q=2.5$ Å$^{-1}=1.426k_F$. There is a fair amount of scatter in the experimental data and observations do not seem to have been made in the low-frequency (0–5 eV) and high-frequency (>45 eV) regions. Again we find that our peak position is practically the same as in FO, while the intensity is somewhat higher. Although this trend is certainly in the right direction, our theoretical curve does not follow the experimental points as closely as could be hoped for. Figure 4(c) shows the situation at $q=3.0$ Å$^{-1}=1.711k_F$. Although there is a considerable amount of scatter in the data, the mean experimental intensity is well above the calculated in any of the theories. We find this fact puzzling and feel it needs further clarification. However, if we ignore the difference in intensities and look at peak positions (taking the experimental peak position from Batson's estimate), we find once again that neither at this q nor at any other q do we see any evidence for the "two-peak" structure in $S(q\omega)$ reported earlier by Platzman and Eisenberger.[15]

In Table III we summarize our calculations for the loss functions by listing its peak position and maximum intensity (i.e., intensity at the peak position) for a wide range of momentum transfers. The different entries shown in the table are for (1) RPA, (2) the first-order theory of I, referred to here as FO, and (3) present theory with *Ansatz A*. For $r_s=2.0$, the experimental peak positions of

TABLE III. Peak position and maximum intensity of $\mathrm{Im}[-1/\epsilon(q\omega)]$ in different theories.

r_s	q (units of k_F)	Peak position (in units of $E_F/\hbar$)			Maximum intensity		
		RPA	FO	GRPA	RPA	FO	GRPA
2.0	0.9	2.40	1.89	1.90	1.76	1.07	1.38
	1.0	2.59	2.03	2.01	1.04	0.81	0.98
	1.2	2.90	2.27	2.26	0.54	0.50	0.56
	1.4	3.21	2.55	2.48	0.34	0.33	0.36
	1.6	3.59	2.94	2.80	0.24	0.23	0.25
	1.8	4.08	3.45	3.25	0.17	0.17	0.18
	2.1	5.04	4.44	4.17	0.11	0.11	0.11
	2.5	6.69	6.12	6.01	0.07	0.07	0.07
	3.0	9.30	8.75	8.68	0.04	0.04	0.04
4.0	1.2	3.48	2.52	2.61	1.46	1.05	1.87
	1.4	3.90	2.84	2.81	0.74	0.66	0.91
	1.8	4.75	3.63	3.39	0.33	0.33	0.38
	2.1	5.60	4.49	4.09	0.21	0.22	0.23

Batson are only slightly lower than those of FO (see Fig. 7.4 of I). This table reinforces the comments made earlier about the loss function in our theory: the peak positions are practically the same as in FO while the intensities are somewhat higher. Both these trends are confirmed by experiment. In the lower part of the table we have shown our results for Na ($r_s=4.0$) at some momentum transfers where the plasmon is no longer a well-defined excitation. We hope that our results will serve as a spur to the experimentalists to measure the detailed line shapes at these larger momentum transfers.

In Table IV we show the static structure factors calculated in the different theories discussed above. In the last column we have shown the structure of Vashishta and Singwi (VS), which has been taken as an input in our calculation. It is interesting to note, on comparing the last two columns, that our theory is almost "self-consistent" in that the difference between our calculated $S(q)$ and that of VS is less than 3% on the average. On the other hand, a qualitative difference between the two $S(q)$'s is that ours exhibits a slight but definite maximum around $q\sim 2.5$. This tendency happens to be in ac-

TABLE IV. Structure factor $S(q)$ calculated in different theories.

r_s	q (units of k_F)	Structure factor $S(q)$			
		RPA	FO	GRPA	VS
2.0	0.9	0.428	0.44	0.42	0.453
	1.0	0.497	0.51	0.53	0.527
	1.2	0.626	0.670	0.681	0.668
	1.4	0.741	0.790	0.805	0.789
	1.6	0.835	0.891	0.907	0.883
	1.8	0.904	0.959	0.976	0.947
	2.1	0.953	0.986	1.001	0.982
	2.5	0.977	0.991	1.002	0.993
	3.0	0.989	0.995	1.001	0.997
4.0	1.2	0.537	0.52	0.57	0.597
	1.4	0.655	0.721	0.77	0.734
	1.8	0.840	0.924	0.957	0.926
	2.1	0.912	0.968	1.005	0.976

cord with the recent x-ray scattering experiments of Eisenberger *et al.*,[16] where a rather pronounced maximum in $S(q)$ is observed at the same wave vector. This point needs further theoretical consideration, i.e., inclusion of multiple particle-hole pairs.

XI. CONCLUSION

Before reviewing the overall performance of our theory, we would like to recall briefly the motivations that led to it. Our aim has been to formulate a microscopic theory of dynamical correlations which incorporates explicitly the role of the multipair excitations. In order to do this we felt it would be fruitful to begin from the exact quantum kinetic equation for the two-particle distribution function because (a) it provides a rigorous basis for studying the dynamics of two-coupled particle-hole excitations and (b) the various terms occurring in it have a simple semiclassical interpretation. The latter aids greatly in a visualization of the physical processes involved, which is necessary if one is to develop suitable approximation schemes. By making an RPA-like truncation of this equation and using the result in the exact one-particle kinetic equation, we were able to obtain a simple expression for the density-density response function in the present theory.

In order to obtain numerical results on the basis of this approach, we made the approximative *Ansätze A* and *B* for the equilibrium correlation function $f^{(2)}$. Our polarizability was then expressible in the form $Q=Q^0+Q^1+Q^h$, where the contributions arise, respectively, from RPA, first-order perturbation theory (FO), and higher-order correlation effects. In comparing our theory with experiment, we shall first confine our remarks to Al ($r_s=2.0$). The positive achievements of our theory are as follows: (1) The correction Q^h gives rise to a damping of the plasmon at long wavelengths, which was lacking in both RPA and FO. We find that the width of the plasmon is proportional to q^2. Our numerical estimate of the plasmon dispersion is in good agreement with the data for Al, while the width is half the experimental value. (2) There is an enhancement of the compressibility over RPA and FO coming from Q^h, and we find that the compressibility sum rule is remarkably well satisfied for $r_s \leq 2$. (3) There is a considerable shift towards lower energy in the peak position of the energy-loss function and the latter is in good agreement with the experiment. (4) The absolute value of the intensity of the loss function is much closer to the experiment than in first-order theory. (5) There is a high-frequency tail in $S(q\omega)$ due to multipair excitations. (6) A small but definite peak is observed in $S(q)$ at $q\simeq 2.5$. Our calculations show that *Ansatz A* leads to much better results than *Ansatz B*.

The negative features of the theory are as follows: (1) It fails to remove the singularities at $\omega_s=|(q^2/2)\pm q|$ present in FO and therefore, like FO, becomes invalid in the vicinity of these frequencies. (2) As a consequence of (1), $S(q\omega)$ becomes slightly negative around this region. For q close to the critical wave vector q_c, this negative portion is quite pronounced and the theory becomes completely unreliable. However, if we stay away from the dangerous frequency regions around ω_s (for a given q), the theory is seen to be in good overall agreement with experiment.

For $r_s=4.0$, the predictions of the theory are not satisfactory. Because of enhanced correlation effects the terms Q^1 and Q^h are much larger in relation to Q^0 than they are for $r_s=2.0$. This leads us to infer that the role of the terms we have neglected in our theory may be quite significant at lower densities ($r_s>2$). If this is indeed the case, our theory would have a quasiperturbative character and its validity would be best confined to the high-density region $r_s \lesssim 2$.

In attempting to improve the present theory, the major objective should be to remove the unphysical behavior present in the vicinity of the characteristic frequencies ω_s. Unfortunately, we know of no precise criterion which tells us which additional terms to retain in the equation of motion in order to accomplish this objective, and even if such a criterion existed, it might not prove possible to implement in practice. One new physical effect arising from some of the neglected terms in the two-particle equation is a renormalization of the free-particle energy denominators occurring in our theory. Although this effect can be demonstrated in a straightforward manner, the problem is again of incorporating it into the theory in a tractable way. For $r_s=2.0$, we feel that these extra sophistications will serve only to patch up our theory near ω_s, while leaving it essentially unaltered at other frequencies. For $r_s>2$, however, the present approach becomes increasingly inadequate, and it is clear that much work remains to be done on the problem of including higher-order correlation effects in a low-density electron gas.

ACKNOWLEDGMENTS

This work was supported in part under National Science Foundation-Materials Research Laboratories program through the Material Research Center of Northwestern University (Grant No. DMR76-80847) and in part by the National Science Foundation Grant No. DMR77-09937.

---

*Permanent address: Institute of Nuclear Research, Swierk, 05-400 Otwock, Poland.

[1]A. Holas, P. K. Aravind, and K. S. Singwi, Phys. Rev. B 20, 4912 (1979).

[2]D. J. W. Geldart and R. Taylor, Can. J. Phys. 48, 155 (1970).

[3]P. E. Batson, C. H. Chen, and J. Silcox, Phys. Rev. Lett. 37, 937 (1976). Also, P. E. Batson, thesis, Cornell University, 1976 (unpublished).

[4]G. Niklasson, Phys. Rev. B 10, 3052 (1974).

[5]K. S. Singwi, M. P. Tosi, R. H. Land, and A. Sjolander, Phys. Rev. 176, 589 (1968).

[6]P. Vashishta and K. S. Singwi, Phys. Rev. B 6, 875 (1972).

[7]P. K. Aravind, Ph.D. thesis, Northwestern University, 1979 (unpublished).

[8]See L. P. Kadanoff and G. Baym, in *Quantum Statistical Mechanics* (Benjamin, New York, 1976), p. 35.

[9]P. C. Gibbons, S. E. Schnatterly, J. J. Ritske, and J. R. Fields, Phys. Rev. B 13, 2451 (1976).

[10]D. F. DuBois, Ann. Phys. (N.Y.) 8, 24 (1959).

[11]D. F. DuBois and M. G. Kivelson, Phys. Rev. 186, 409 (1969); see also A. J. Glick and W. F. Long, Phys. Rev. B 4, 3455 (1971).

[12]M. Hasagawa and M. Watabe, J. Phys. Soc. Jpn. 27, 1393 (1969).

[13]B. W. Ninham, C. J. Powell, and N. Swanson, Phys. Rev. 145, 209 (1966).

[14]M. Hasegawa, J. Phys. Soc. Jpn. 31, 649 (1971).

[15]P. M. Platzman and P. Eisenberger, Phys. Rev. Lett. 33, 152 (1974).

[16]P. Eisenberger, W. C. Marra, and G. S. Brown, Phys. Rev. Lett. 45, 1439 (1980).